Journal of Zhejiang University SCIENCE A
ISSN 1673-565X (Print); ISSN 1862-1775 (Online)
www.zju.edu.cn/jzus; www.springerlink.com
E-mail: jzus@zju.edu.cn

Strengthening an in-service reinforcement concrete bridge with prestressed CFRP bars*

Hai-long WANG†1, Wei-liang JIN[1], David J. CLELAND[2], Ai-hui ZHANG[1]

([1]*Department of Civil Engineering, Zhejiang University, Hangzhou 310027, China*)

([2]*School of Planning, Architecture and Civil Engineering, Queen's University Belfast, Belfast BT9 5AG, UK*)

†E-mail: hlwang@zju.edu.cn

Received Dec. 3, 2008; Revision accepted Mar. 23, 2009; Crosschecked Feb. 19, 2009

Abstract: Carbon fiber reinforced polymer (CFRP) bars were prestressed for the structural strengthening of 8 T-shaped reinforced concrete (RC) beams of a 21-year-old bridge in China. The ultimate bearing capacity of the existing bridge after retrofit was discussed on the basis of concrete structures theory. The flexural strengths of RC beams strengthened with CFRP bars were controlled by the failure of concrete in compression and a prestressing method was applied in the retrofit. The field construction processes of strengthening with CFRP bars—including grouting cracks, cutting groove, grouting epoxy and embedding CFRP bars, surface treating, banding with the U-type CFRP sheets, releasing external prestressed steel tendons—were introduced in detail. In order to evaluate the effectiveness of this strengthening method, field tests using vehicles as live load were applied before and after the retrofit. The test results of deflection and concrete strain of the T-shaped beams with and without strengthening show that the capacity of the repaired bridge, including the bending strength and stiffness, is enhanced. The measurements of crack width also indicate that this strengthening method can enhance the durability of bridges. Therefore, the proposed strengthening technology is feasible and effective.

Key words: Carbon fiber reinforced polymer (CFRP) bar, Reinforced concrete (RC) bridge, Strengthening, Construction procedure, Field test, T-shaped beam

doi:10.1631/jzus.A0820836 **Document code:** A **CLC number:** TV4

INTRODUCTION

A number of structural members which are part of the concrete infrastructure are in serious need of strengthening or repair to restitute their service capacities in strength and ductility due to aging, damage from overloading, impact of over-height vehicles, corrosion of steel rebar, and deterioration of concrete, or as a result of the demand for higher design loads, improved serviceability requirements, or the correction of poor design or construction. Recent surveys suggested that the necessary strengthening or repair for bridges, especially those exposed to the aggressive environments and/or those on strategically important routes, had led to increasing maintenance costs in the past decades (GB 50367, 2006; Capozucca, 2007).

To improve the overall capacity of concrete bridges, many techniques have been employed in the strengthening. Of these methods, externally post-tensioned steel tendons, bonding steel plates and attaching fiber reinforced polymers (FRP) sheet to the concrete surface are popular strengthening methods for in situ construction because of their advantages (Ross *et al*., 1999; Shahawy *et al*., 2001; GB 50367, 2006). However, their shortcomings are also obvious, such as the corrosion of steel and interface, adding negative load especially in the long-span structures repaired with steel, premature local failures, and not taking full advantage of material strength. Recently a

* Project supported by the National Hi-Tech Research and Development (863) Program of China (No. 2007AA04Z437), the National Natural Science Foundation of China (No. 50808158), the Zhejiang Provincial Natural Science Foundation of China (No. Y107049)

potential solution to some of these problems with FRP bars has attracted attention because of its favorable weight-to-strength ratio, non-corrosion, high resistance to chemicals, lighter, and more durable than alternative repair systems (Quantrill and Hollaway, 1998). And some researchers investigated FRP bars as a promising alternative to conventional steel reinforcement in concrete structures (Abdalla, 2002; Rasheed *et al*., 2004; Nayal and Rasheed, 2006). Based on the present studies, several codes and design guidelines have been published in the past few years, such as ISIS-M03-01 by Intelligent Sensing for Innovative Structures (ISIS) Canada, ACI 440.1R-03 by American Concrete Institute (ACI), to encourage the construction and design of concrete structures with FRP bars. For example, Engineers in Canada used glass FRP bars as reinforcement in the concrete deck slab of one full span to construct the Cookshire-Eaton Bridge (El-Salakawy *et al*., 2005). The use of FRP bars as reinforcement in the deck construction of Pierce Street Bridge and Ohio's Salem Avenue Bridge in USA has been reported (ACI 440, 2003).

Nevertheless, most of the research projects were performed with laboratory-scale tests and corresponding analyses. The corresponding codes and guidelines were published just for the design of concrete structures using FRP bars alone instead of alongside steel reinforcement in the tension zone, while reports of field applications of strengthening reinforced concrete (RC) structures with FRP bars are limited. Existing investigations showed that CFRP bar has excellent fatigue characteristics as it survived 2×10^6 cycles when used in prestressed concrete beams and showed no reduction in the tensile capacity (Abdelrahman and Rizkalla, 1997). If it can be used in strengthening, a favorable effect can be achieved. Ha *et al*.(2008) developed a technique by embedding high-performance CFRP trapezoidal bars into grooves in the concrete to reinforce a beam in the laboratory. This proposed strengthening method was validated via a comparison with the performance of conventionally strengthened beams, showing that this method made significant improvements in ductility and load-carrying capacity of concrete beams (Ha *et al*., 2008). Recently, several attempts have deployed CFRP bar as external post-tensioning tendons to strengthen structures (Matta *et al*., 2007; Fang *et al*., 2008), showing that external prestressed CFRP tendons improved the bending capacity of beams and reduced the deformation and crack width. However, this challenge needed a special treatment to the CFRP bar and anchor systems. The transverse mechanical properties of CFRP are typically two orders of magnitude smaller than those in the direction of the fiber (Matta *et al*., 2007). Without special treatment, the CFRP bar in the anchor will be crushed easily and also, the rupture of the CFRP bar often happens on the turning point (Fang *et al*., 2008).

To overcome some difficulties in the external prestressed method, this study develops a novel strengthening method using prestressed CFRP bars embedded in the groove to repair a 21-year-old RC bridge in service. The design of the repair, field application, in-situ tests, analytical investigations, and an assessment on the effectiveness of this strengthening method are also discussed.

ANALYSIS AND DESIGN

Bridge service condition

The Erhutou Bridge, located in Huzhou City of Zhejiang Province, China, is a single span beam bridge with 8 main T-shaped RC beams. Note that the span of those RC beams is 16 m, and the width of the flanges of the T-shaped beams is 1.60 m (for the cross section of this bridge, refer to Fig.1). Since its construction in 1986, this bridge has been in service for 21 years.

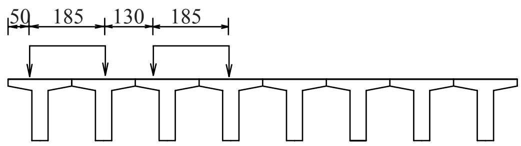

Fig.1 Cross section of the strengthened bridge (unit: cm)

Concomitant with aging and the increasing traffic, overload and environmental deterioration have caused different degrees of damage to this bridge (Fig.2). As shown in Fig.3, serious cracks appeared in the edge beams, and water seeping from cracks in the pavement brought further durability problems to the bridge beams. Corrosion of steel bars and

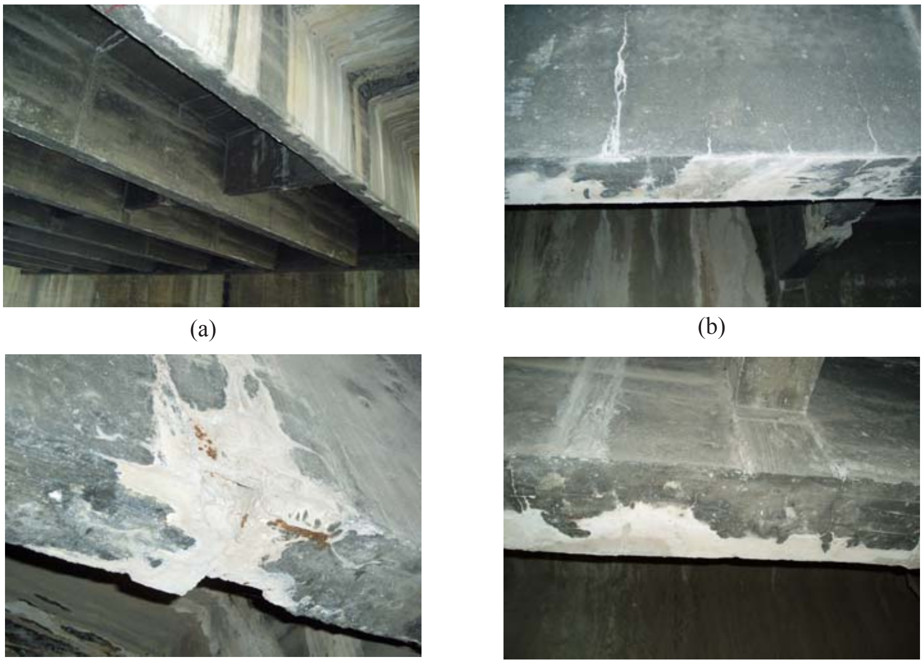

(a) (b) (c) (d)

Fig.2 Damages of RC bridge. (a) Leakage; (b) Cracking; (c) Corrosion of steel and spalling of concrete; (d) Leakage and cracking

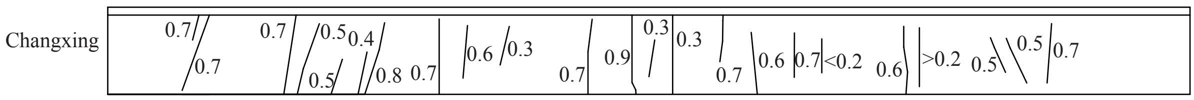

Fig.3 Width and distribution of cracks in the edge beam (Beam 1) (unit: mm)

plates in the diaphragm led to concrete cover spalling from the members, which in turn loosened the joint connection of two diaphragms to the main beams (Fig.2d). As a result, beams vibrated severely when vehicles passed through the bridge. Our inspection and evaluation of the results showed that the deterioration in the bridge had a considerable impact on the security of structures, and retrofit was urgently required.

Material characteristics

CFRP bars at the diameter of 10 mm (Fig.4) were adopted to strengthen the T-shaped beams. When loaded in tension, these bars exhibit a linearly elastic stress-strain relationship until rupture. Their tensile properties, including ultimate tensile strength f_p and elastic modulus E_p, are summarized in Table 1.

The C-30 CFRP sheet was used in this retrofit to ensure the bonding property of CFRP bars and shear strength of the beam. The density of CFRP sheet is 300 g/mm^3 with a thickness of 0.167 mm. The main mechanical properties of this material including the tensile strength f_{ts}, elastic modulus E_{ps}, and elongation percentage L_p are also shown in Table 1.

Fig.4 10-mm diameter CFRP bar

Epoxy resin was used as the adhesive material between concrete and CFRP bar. The tensile bond strength is above 3.5 MPa, larger than the tensile strength of concrete.

The A3 steel plates at a thickness of 10 mm and a

Table 1 Mechanical properties of materials

Material	Parameter	Value	Material	Parameter	Value
CFRP bar	D (mm)	10	Concrete	f_{cu} (MPa)	30
	f_p (MPa)	2760		E_c (GPa)	30
	E_p (GPa)	110	A3 steel plate	f_{yp} (MPa)	235
C-30 CFRP sheet	f_{ts} (MPa)	3430		E_{sp} (GPa)	199
	E_{ps} (GPa)	230	Steel rebar	f_y (MPa)	335
	L_p (%)	1.5		E_s (GPa)	200

D: diameter of CFRP bar; f_p: tensile strength of CFRP bar; E_p: elastic modulus of CFRP bar; f_{ts}: tensile strength of CFRP sheet; E_{ps}: elastic modulus of CFRP sheet; L_p: elongation percentage of CFRP sheet; f_{cu}: compressive strength of concrete; E_c: Young's modulus of concrete; f_{yp}: yield strength of A3 steel plate; E_{sp}: elastic modulus of A3 steel plate; f_y: yield strength of steel rebar; E_s: elastic modulus of steel rebar

width of 200 mm were employed to strengthen the diaphragm. Their yield strength f_{yp} and elastic modulus E_{sp} are presented in Table 1.

The compressive strength f_{cu} and Young's modulus E_c of structural concrete and the yield strength f_y and elastic modulus E_s of steel rebar are also given in Table 1.

Strength analysis

The inspection showed that the serviceability of this bridge was not adequate in terms of the cracks, corrosion and vibration; meanwhile, the owner suggested improving the load-carrying capacity of the bridge to meet the increasing volume traffic. In order to enhance the durability and load-carrying capacity of the RC bridge, a strengthening solution was designed.

The bending capacity of the T-shaped beams was analyzed by assuming that the plane sections remain plane until failure. Dimensions of the T-shaped beam cross section and meanings of the symbols are shown in Fig.5. The bearing strength of the beam M_u equals to 1708 kN·m.

Due to the excellent bonding strength, the failure of the beam strengthened with CFRP bars will be flexural failure. The flexural capacity of a CFRP bar strengthened member is dependent on whether the failure is governed by concrete crushing or CFRP rupture. In terms of Fig.5 and the plane sections assumption, the bending capacity of beams strengthened with CFRP bars were analyzed according to the two failure modes.

In terms of the strain compatibility in Fig.5, the strain of steel bar ε_s can be expressed by

$$\varepsilon_s = \frac{h_s - x_c}{h_p - x_c}\varepsilon_p, \quad (1)$$

where h_s denotes the depth from the top of the section to the centroid of tensile steel rebars, h_p refers to the depth from the top of the section to the centroid of CFRP bars, x_c is the neutral axis depth, and ε_p represents the strain of CFRP bars. When CFRP rupture failure happens, ε_s goes beyond the allowance strain of steel rebars, which is 0.01 according to China Design Code of Concrete Structure (GB 50010, 2002). Therefore, the failure is not governed by steel yielding.

When concrete crushing failure happens, the ultimate value of strain for compressive concrete ε_{cu} is

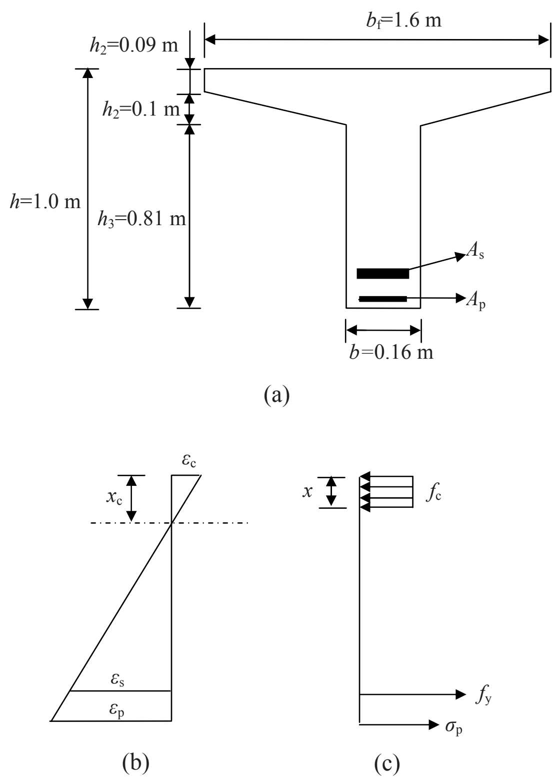

Fig.5 Typical stress and strain distributions along the section of the T-shaped beam with CFRP bars. (a) Cross section of the beam; (b) Strain distribution; (c) Stress distribution

assumed equal to 0.003, and ε_s is larger than the yield strain of steel rebar and smaller than 0.01 from the relationship of strains between concrete and steel rebar. The strain of CFRP bars can be obtained as follows in terms of the concrete strains:

$$\varepsilon_p = \frac{h_p - x_c}{x_c} \varepsilon_{cu}. \tag{2}$$

Since CFRP is a linearly elastic material, the stress of CFRP bars σ_p can be calculated by:

$$\sigma_p = E_p \varepsilon_p + \sigma_{pe}, \tag{3}$$

where σ_{pe} is the prestress in CFRP bars.

The standard equations of equilibrium are listed in Eqs.(4) and (5), and from a combination of Eqs.(3)~(5) the bending capacity of the beams after strengthening can be calculated.

$$\alpha_1 f_c b_f x = f_y A_s + \sigma_p A_p, \tag{4}$$

$$M_u = \sigma_p A_p \left(h_p - \frac{x}{2} \right) + f_y A_s \left(h_s - \frac{x}{2} \right), \tag{5}$$

where x=0.8x_c, α_1=1.0, A_s is the area of tensile steel reinforcement, A_p is the area of CFRP bars, and M_u is the flexural strength of the T-shaped beams strengthened with CFRP bars.

According to the above analysis, the ultimate bending strength was controlled by the failure of concrete crushing when the beam was strengthened with CFRP bars. The bending strength of the T-shaped beam is 1961.2 kN·m when reinforced with 2 CFRP bars, which satisfies the requirement of design loading.

STRENGTHENING PROCEDURE WITH CFRP BARS

The construction procedure of RC beams strengthened with CFRP bars was performed as follows:

(1) Grouting cracks: Cracks in the T-shaped beams were sealed by a chemical grouting method.

(2) Cutting Grooves in the concrete cover: In order to obtain a good interface between concrete and the CFRP U-shaped plate, the concrete surface was removed. Then, longitudinal grooves were formed in the concrete cover. The surfaces of the grooves were prepared with a wire brush to remove the loose concrete and dirt; four grooves formed in each edge beam and two grooves in every interior beam. Before the installation, compressed air at more than 0.2 MPa pressure was adopted to blow the dirt from the grooves, and the concrete surface was scrubbed cleanly with acetone.

(3) Prestressing the beams: Counterforce piers and anchors were prefabricated and fixed at the end of each side of the T-shaped beams. External steel tendons, at a diameter of 15.2 mm, were prestressed with 150 kN tension using a hydraulic jack.

(4) Grouting with epoxy adhesive: the epoxy adhesive material was mixed and then the epoxy resin was grouted into the rebates after the application of the primer in the concrete. Before the in situ application, bond performance was tested in the laboratory.

(5) Embedding CFRP bars: The surfaces of the CFRP bars were made rough, cleaned and coated with sand. Then these CFRP bars were embedded into the epoxy filled rebates, and surplus adhesive epoxy resin was removed.

(6) Fixing the CFRP sheet: To protect and strengthen the interface, the U-shaped sheet of CFRP with a thickness of 0.167 mm was bonded on the concrete surface of the strengthened beam. The contribution of this sheet was deemed as a safety stock and not taken into account in the strength calculations.

(7) Releasing the external prestressing tendons: The prestress in the external steel tendon was released when the bond strength between the CFRP bar and concrete achieved a satisfactory result with reference to the laboratory test. In this way, the CFRP bar would be stressed before live loading.

The main strengthening steps are shown in Fig.6. After the above strengthening procedure, steel plates were bonded on the diaphragms, and deck slab topping was recast to enhance the transverse interaction between the beams. The steel plates were also protected with special paint to ensure their durability.

LIVE LOAD TEST IN SITU

Field test program

Before retrofit and after 5 months before re-opening to the traffic, the service performance of this bridge was tested using calibrated vehicles as live loads (for the detail of the vehicles, refer to Fig.7). To guarantee the security of this bridge, the vehicular loads were applied and removed from the bridge deck according to different stages shown in Table 2. And four vehicle stations were distributed in the deck (Fig.8).

In the first stage of the test, vehicle 1 (V_1) and vehicle 2 (V_2) stopped on the marked station. In the second stage, vehicle 3 (V_3) was added and subsequently vehicle 4 (V_4) was added (the third stage). After the third stage, vehicular loads were removed according to the sequence described in Table 2. The gross rail loads on axles of vehicles before and after strengthening are listed in Table 3. The readings of

Table 2 Stage and sequence of loading and unloading calibrated vehicles

Stage	Sequence	Stage	Sequence
0	0	4	$V_1+V_2+V_3$
1	V_1+V_2	5	V_1+V_2
2	$V_1+V_2+V_3$	6	0
3	$V_1+V_2+V_3+V_4$		

Note: stages 0~3: loading calibrated vehicles; stages 4~6: unloading calibrated vehicles

Table 3 Gross rail loads on axles of vehicles before and after strengthening

Vehicle		Fore axle t_1 (t)	Back axle t_2 (t)	Back axle t_3 (t)
Before strengthening	V_1	57.80	128.39	128.39
	V_2	49.22	132.19	132.19
	V_3	53.33	130.63	130.63
	V_4	57.22	126.57	126.57
After strengthening	V_1	65.53	114.53	114.53
	V_2	39.20	128.19	128.19
	V_3	59.12	117.49	117.49
	V_4	57.18	118.21	118.21


(a)


(b)


(c)


(d)


(e)

Fig.6 Main construction steps in the strengthening site. (a) Cutting the groove; (b) Prestressing the beam; (c) Grouting and embedding; (d) Closing the groove; (e) Hooping with the U-type CFRP sheet

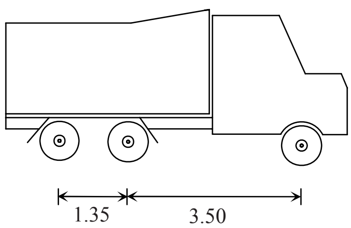

(a)

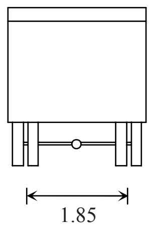

(b)

Fig.7 Vehicle (unit: m). (a) Side view; (b) Back view.

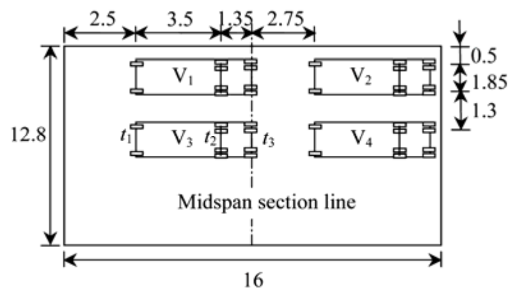

Fig.8 Distribution of vehicular loads on the bridge deck (unit: m)

instrumentations were collected when the data were steady for 30 min after the vehicles stopped at the prescribed stations.

Deflection measurement

Dial indicators were installed on the bottom of the T-shaped beams to measure the deflection. The midspan deflection at each test load stage is shown in Figs.9a and 9b for 4 beams before and after structural strengthening, respectively.

It can be seen from the curves between deflection and loads in Fig.9a, the vehicular loads on the deck do not distribute to every beam according to theoretical model because of the weak transverse interaction between the beams. Before strengthening, the maximum deflection of the edge beam (Beam 1) under the 3rd stage load was 1.24 cm. After strengthening, the maximum deflection of Beam 1 at the same stage was 0.95 cm.

Strain measurement

Foil gauges were attached to the bottom concrete surface and to the CFRP bars at the midspan section to monitor their strains. The strains were collected with an acquisition system at a rate of two readings per second. Unfortunately, the foil gauges on the CFRP bars were destroyed in the strengthening construction, and some interesting data were not collected.

Figs.10a and 10b show the concrete strains under vehicular loads before and after strengthening, respectively. Compared with other beams, the strain is the greatest in the edge beams. The maximum strain

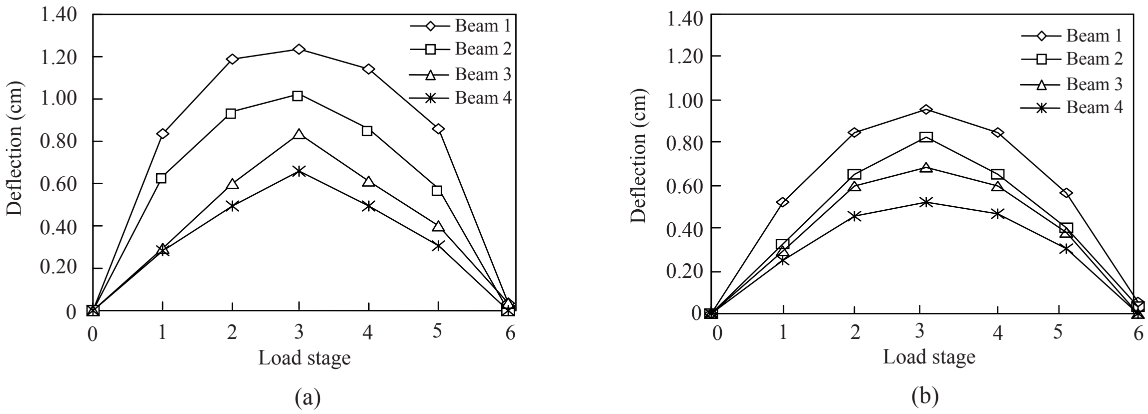

Fig.9 Midspan deflection vs load stage curves (a) before and (b) after strengthening

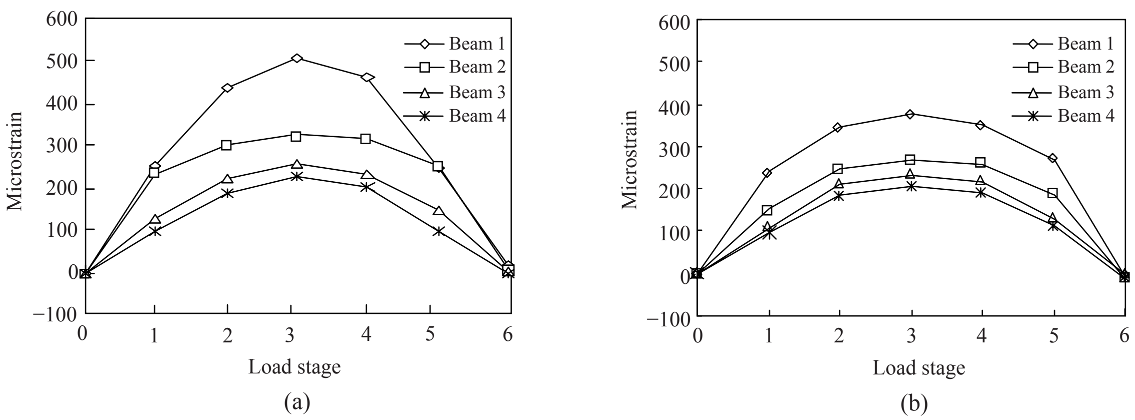

Fig.10 Concrete strain vs load stage curves (a) before and (b) after strengthening

of the edge beam under the 3rd stage load before strengthening was 508 microstrain due to the damage and the weak interaction between the beams. Here, the width of some cracks is much larger than that is desirable for durability of concrete structures. After strengthening, the strain was reduced; the maximum strain of edge beam under the 3rd stage load now was 379 microstrain.

Cracks

In the load test of the bridge before retrofitting the width of the cracks in the concrete increased with the loading, but no new cracks appeared. These cracks had affected the durability of the structure and would have further decreased the performance of the bridge if no action were taken. In order to monitor the development of cracks after retrofit, a repaired crack in the midspan of Beam 2, with a width of 0.2 mm before retrofit, was selected as a monitoring object in the field test. Its width was unchanged under the first stage load, 0.03 mm under the second stage load, 0.05 mm under the third stage load, and closed when the live loads were removed from the bridge deck. Furthermore, after reopening to the traffic, periodical inspections were carried out on three occasions to observe the development of surface cracks on the sides of the beams. The cracking was found to be stable.

EVALUATION AND DISCUSSION

Live load distribution factor

The live load distribution factor (*DF*) is by definition the fraction of the total load that anyone of the T-beams receives. By measuring the deflection of every beam in the bridge under static loading, the *DF* can be determined. Since all of the T-shaped beams have nearly the same dimensions, the stiffness of these beams can be considered approximately as the equal value. The following equation can thus be adopted to calculate the *DF*s in the test (Eom and Novak, 2001):

$$DF_i = f_i / \sum f_i, \tag{7}$$

where f_i is the deflection of the ith beam, i=1~8.

The *DF*s from Beam 1 to Beam 4 are shown in Fig.11. Through the comparison, the theoretical rigid-diaphragm method (JTGD60, 2004) is valid to evaluate the *DF*s of the T-shaped beam bridge after retrofit.

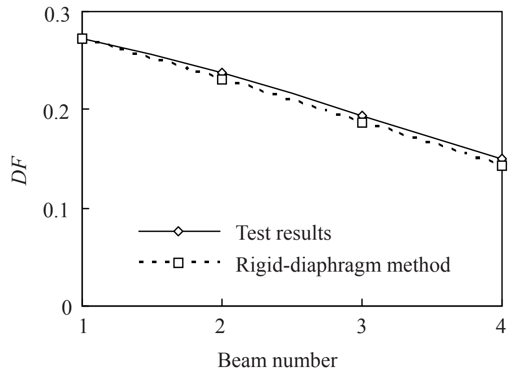

Fig.11 Live load distribution factors calculated from test results and rigid-diaphragm method

Effectiveness of the strengthening

Because the test loads at the same stage before and after strengthening are slightly different, the relative ratio of f_i/f' was put forward to evaluate the effectiveness of this strengthening. In the above ratio f_i is the deflection of the ith beam observed from the test and f' is the deflection calculated from the equation adopted by ACI 318 (2002). When cracking occurs, the moment of inertia or the stiffness of the beam decreases. For cracked concrete, an effective moment of inertia I_e used for the calculation of deflection can be expressed as (ACI, 2002)

$$I_e = \left(\frac{M_{cr}}{M_a}\right)^3 I_g + \left[1 - \left(\frac{M_{cr}}{M_a}\right)^3\right] I_{cr} \le I_g, \tag{8}$$

where I_g is the gross (uncracked) moment of inertia, I_{cr} represents the cracked transformed moment of inertia, M_{cr} denotes the cracking moment of the beam, and M_a refers to the applied service load moment at the critical section.

The values of f_i/f' before and after strengthening are shown together in Fig.12. It can be seen that the bridge structure has been stiffened by using CFRP bars and retrofitting the deck slab. All of the f_i/f' values after strengthening are less than 0.73, so the bridge performance is better than what the design code assumes.

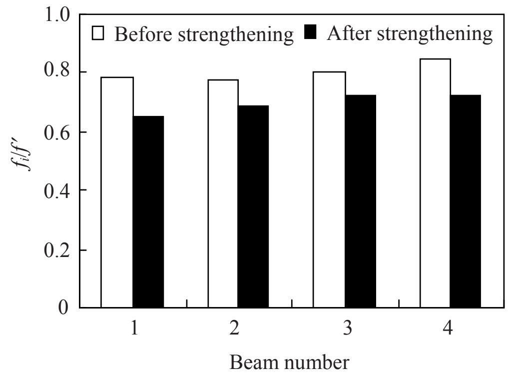

Fig.12 Effectiveness evaluation of the strengthening with CFRP bars

CONCLUSION

An innovative strengthening technology is described to improve the flexural strength and serviceability of a 20-year-old RC bridge with prestressed CFRP bars. The detailed construction procedure on site is also reported. Field tests were carried out to evaluate the performance of this RC bridge in its existing state and the effectiveness of our repair method. Based on the analysis and the results of a field test, some conclusions can be drawn as follows:

(1) The flexural strength of RC members strengthened with CFRP bars can be determined based on strain compatibility, internal force equilibrium, and the controlling mode of failure. It has been shown that the flexural strength of the T-shaped beams strengthened with CFRP bars is governed by concrete crushing;

(2) The bending capacity of the damaged bridge was improved by embedding the prestressed CFRP bars in the tensile zone of beams. The deflection and crack width was reduced after the retrofit, and thereby the durability of the concrete beams has been improved;

(3) The transverse interaction between bridge beams has been improved by the retrofit of diaphragms and deck slab. The live load distribution factors of the strengthened bridge calculated from experimental results were in good agreement with the rigid-diaphragm method;

(4) The construction work on site has demonstrated that the proposed strengthening method is feasible and effective.

References

Abdalla, H.A., 2002. Evaluation of deflection in concrete members reinforced with fiber reinforced polymer (FRP) bars. *Composite Structures*, **56**(1):63-71. [doi:10.1016/S0263-8223(01)00188-X]

Abdelrahman, A.A., Rizkalla, S.H., 1997. Serviceability of concrete beams prestressed by carbon fiber reinforced plastic bars. *ACI Structural Journal*, **94**(4):447-457.

ACI (American Concrete Institute Committee) 318, 2002. Buliding Code Requirements for Structural Concrete and Commentary. ACI 318-02, Farmington Hills, MI, USA.

ACI (American Concrete Institute Committee) 440, 2003. Guide for the Design and Construction of Concrete Reinforced with FRP Rebar. ACI 440.1R-03, Farmington Hills, MI, USA.

Capozucca, R., 2007. Analysis of the experimental flexural behavior of concrete beam grid reinforced with CFRP bars. *Composite Structures*, **79**(4):517-526. [doi:10.1016/j.compstruct.2006.02.011]

El-Salakawy, E., Benmokrane, B., Ragaby, A., Nadeau, D., 2005. Filed investigation on the first bridge deck slab reinforced with glass FRP bars constructed in Canada. *Journal of Composites for Construction*, **9**(6):470-479. [doi:10.1061/(ASCE)1090-0268(2005)9:6(470)]

Eom, J., Novak, A.S., 2001. Live load distribution for steel girder bridge. *Journal of Bridge Engineering*, **6**(6): 489-497. [doi:10.1061/(ASCE)1084-0702(2001)6:6(489)]

Fang, Z., Li, H.F., Peng, B., 2008. Mechanical behaviors of concrete beam of external prestressed CFRP tendons. *China Journal of Highway and Transport*, **21**(3):40-47 (in Chinese).

GB 50010, 2002. Design Codes of Concrete Structures. Ministry of Construction of China, Beijing.

GB 50367, 2006. Strengthening Design Codes of Concrete Structures. Ministry of Construction of China, Beijing.

Ha, G.J., Kim, Y.Y., Cho, C.G., 2008. Groove and embedding techniques using CFRP trapezoidal bar for strengthening of concrete structures. *Engineering Structures*, **30**(4): 1067-1078. [doi:10.1016/j.eng-struct.2007.07.006]

JTG D60, 2004. General Specification for Highway Bridge and Culvert Design. Ministry of Communications of China, Beijing.

Matta, F., Nanni, A., Abdelrazaq, A., Gremel, D., Koch, R., 2009. Externally post-tensioned carbon FRP bar system for deflection control. *Construction and Building Materials*, **23**(4):1628-1639. [doi:10.1016/j.conbuildmat.08.002]

Nayal, R., Rasheed, H.A., 2006. Tension stiffening model for concrete beam reinforced with steel and FRP bars. *Journal of Materials in Civil Engineering*, **18**(6):831-841. [doi:10.1061/(ASCE)0899-1561(2006)18:6(831)]

Quantrill, R.J., Hollaway, L.C., 1998. The flexural rehabilitation of reinforced concrete beams by the use of prestressed advanced composite plates. *Composites Science and Technology*, **58**(8):1259-1275. [doi:10.1016/S0266-3538(98)00002-5]

Rasheed, H.A., Nayal, R., Melhem, H., 2004. Response prediction of concrete beams reinforced with FRP bars. *Composite Structures*, **65**(2):193-204. [doi:10.1016/j.comp-struct.2003.10.016]

Ross, C.A., Jerome, D.M., Tedesco, J.W., Mary, L., 1999. Strengthening of reinforced concrete beams with externally bonded composite laminates. *ACI Structural Journal*, **96**(2):212-220.

Shahawy, M., Chaalal, O., Beitelman, T.E., El-Saad, A., 2001. Flexural strengthening with carbon fiber-reinforced full-scale girders. *ACI Structural Journal*, **98**(5):735-743.